Refractometry of microscopic objects using digital holography

Gustafsson, Mats; Sebesta, Mikael

2003

CODEN:LUTEDX/(TEAT-7120)/1-10/(2003)

Refractometry of microscopic objects using digital holography

Mats Gustafsson and Mikael Sebesta

Department of Electroscience
Electromagnetic Theory
Lund Institute of Technology
Sweden

Mats Gustafsson

Department of Electroscience
Electromagnetic Theory
Lund Institute of Technology
P.O. Box 118
SE-221 00 Lund
Sweden

Mikael Sebesta

Neural AB
S-224 75 Lund
Sweden

Editor: Gerhard Kristensson

Abstract

Digital holography has some desirable properties for refractometry of microscopic objects since it gives phase and amplitude information of an object in all depths of focus from one set of exposures. The refractive index of the object can be determined by observation of the movements of the Becke lines between different focus depths. It is also shown that one single phase image provides an independent technique to determine sign of the relief between an object and the surrounding medium.

1 Introduction

Digital holography (DH) can be used to generate three-dimensional images, generate phase images and to extract material parameters [2, 4, 5, 7–9]. This makes it an interesting alternative to conventional microscopy. In this paper, it is shown that DH also is useful in refractometry of microscopic objects.

Measurements of the index of refraction of small inhomogeneous object such as crystals are made with methods such as the Becke line method, the phase contrast method, and the oblique illumination method [6]. These methods are indirect in the way that the index of refraction is determined with the help of a matching mounting medium. The observed light intensity difference between an object and the mounting medium is called the relief [6]. The relief is positive (negative) if the refractive index of the object is higher (lower) than the refractive index of the mounting medium.

In the Becke line method, the sign of the relief is determined by observation of the movements of the Becke lines between different focus depths [6]. The oblique illumination method involves a blocking of a part of the illuminating light in a microscope and observation of the "shadows" generated by the object. Whether the "shadow" is on the dark side of the observable area or on the bright side, the relief between the object and the mounting liquid can be determined [6]. The Phase contrast method uses the greater dispersion of the mounting liquid in determining the index of refraction of an object. The bright or dark "halo" surrounding the object is observed and by changing the wavelength of the illuminating light, the crossing point in the dispersion curves of the mounting liquid and the object is found. Using the wavelength of the crossing point, the index of refraction of the object can be calculated.

In this paper, it is shown that DH can be used in refractometry of microscopic objects in two independent ways. First, in the Becke line method, the sign of the relief is determined by observation of the movements of the Becke lines between different focus depths. Since, the amplitude images on all depth of focus can be computed from one hologram, the DH is well suited for this method. Secondly, a phase image at the depth of focus gives the variation of the optical distance of the illuminating wave and hence an image of the variation of the index of refraction.

Refractometry has applications in many different sciences. The index of refraction is material specific which is useful for identification of different substrates in a blend. In pharmacology, particle size characterization and distribution of chemical

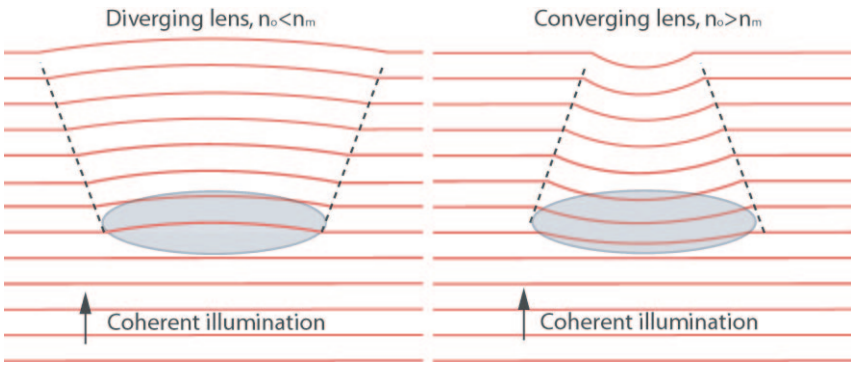

Figure 1: Illustrations of the lens effect when a wave impinges on objects with lower and higher index of refraction than the mounting medium. The horizontal lines show the lines of constant phase for the wave field. The phase of an object with low (high) reflective index is advanced (retarded) and if the object is convex it also acts as an divergent (convergent) lens as depicted to the left (right).

substances play an important role in research and manufacturing. In mineralogy the index of refraction is an important parameter in classifying different minerals [6]. Methods such as the Becke line method and the phase contrast method are widely used in optical mineralogy.

The organization of the paper is as follows. In Section 2, holographic refractometry is described. Experimental results are presented in Section 3. The experimental setup is described in Section 4. Some conclusions are given in Section 5.

2 Holographic Refractometry

When imaging a microscopic object with DH, the interference pattern between the reference field, E_r, and the object field, E_o, is measured on a sensor, *e.g.*, CCD or CMOS sensors. With additional measurements of the object field and the reference field, an approximation of the object field on the sensor is determined as

$$\widetilde{E}_\mathrm{o} = (|E_\mathrm{o} + E_\mathrm{r}|^2 - |E_\mathrm{o}|^2 - |E_\mathrm{r}|^2)/\widetilde{E}_\mathrm{r}^*,$$

where $\widetilde{E}_\mathrm{r}^*$ is the complex conjugate of the assumed known reference field. The object field is focused to an arbitrary plane with numerical computations [4, 7]. At points close to the original position of the object, the amplitude and phase of the object field, $\widetilde{E}_\mathrm{o}$, generate a three dimensional image of the object. This opportunity to generate three dimensional images of the object from one set of exposures is suitable for the Becke line method.

In the Becke line method, the movements of the Becke lines are used to determine whether an object has higher or lower index of refraction than the mounting medium, *i.e.*, positive or negative relief. The Becke lines are observed as bright lines around of the object. When observing image planes just in front of the object, *i.e.*, slightly out

of focus, the Becke lines appears to move into the region with the higher refractive index [6].

The Becke lines are formed by the interference between the scattered wave field of the object and the illuminating wave field. The formation of them is based on the lens effect and the internal reflection effect. Both these effects tend to concentrate the wave field to the region with the higher refractive index. The lens effect is observable for objects that are thinner on the edges than the middle. Such objects acts as converging (diverging) lenses if the object has a higher (lower) refractive index than the surrounding medium, see Figure 1. The internal reflection effect is caused by refraction of rays into (out from) regions with higher (lower) refractive index [6].

The DH gives an additional method to determine the sign of the relief. This independent method is based on the observation that the phase of the image depends on the optical distance for the illuminating wave [1]. If the phase of the illuminating wave is chosen such that it increases in the direction of the propagation, the phase image increases (decreases) in regions with higher (lower) refractive index. This behavior is due to the corresponding increase (decrease) of the optical distance for the illuminating wave in such regions, see Figure 1.

3 Experimental Results

3.1 Oil, water, and air mixture

The digital holographic refractometry is first demonstrated with a sample consisting of an air bubble in immersion oil together with small droplets of water trapped in the air bubble as well as in the oil. The different droplets of water are thus mounted in mediums with higher and lower index of refraction, respectively. In the amplitude images, Figure 2a, the Becke lines can be observed moving into the regions with higher index of refraction as the focus is moved in the direction of the illuminating wave. For the water droplets ($n = 1.33$) in the immersion oil ($n = 1.51$), the Becke lines move out from the droplets as the focus depth is shifted from $-50\,\mu$m to $50\,\mu$m, *i.e.*, the interference fringes are centered inside the water droplets at $-50\,\mu$m whereas the interference fringes are outside the water droplets at $50\,\mu$m. For the water droplets inside the air bubble ($n = 1.00$), the Becke lines move from the surrounding air towards the center of the water droplets as the focus depth is shifted from $-50\,\mu$m to $50\,\mu$m.

In Figure 2b, the phase image of the object is shown when the focus is set on the droplets. The phase increases in the parts of the object with higher index of refraction. This can be seen in the image as circular patterns with higher or lower phase value, *i.e.*, color. In the droplet mounted in oil the color pattern indicates that the phase decreases towards the center of the droplet and the opposite applies for the droplets inside the air bubble. However, due to the large contrast between the refractive indexes, the large objects, and the 2π modulation of the phase it is difficult to resolve the phase images.

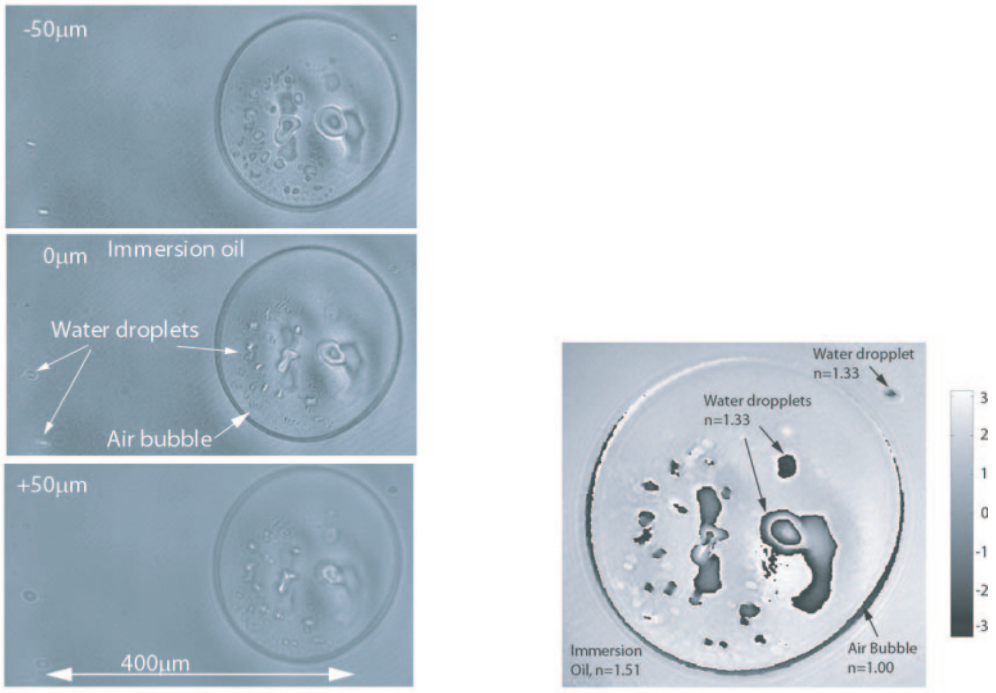

Figure 2: Amplitude and phase images of an oil, water, and air mixture. a) The Becke lines are seen to move into the regions with higher refractive index as the image plane is shifted in the direction of the illuminated wave, *i.e.*, towards the sensor from $-50\,\mu$m to $50\,\mu$m. b) Phase image of an air bubble with water droplets. The phase increases when going from an object with lower refractive index to an object with higher refractive index, *i.e.*, the color changes from black over gray to white and back to black, modulus 2π.

3.2 Lactose crystals

A sample consisting of lactose crystals in a wet mount is secondly used for experimental demonstration of the digital holographic refractometry. The lactose crystals are anisotropic, *i.e.*, the velocity of light depends on direction of propagation [1]. In the DH-system, the anisotropy gives two major effects. First, the linearly polarized wave that illuminates the crystal is transformed into an elliptically polarized wave upon transmission through the crystal. Secondly, the co-polarized part of the transmitted wave appears to have been scattered by an isotropic crystal with an effective refractive index n', where n' is in the range given by the smallest and largest of the principal refractive indexes of the crystal, *i.e.*,

$$\min\{n_{\text{lactose}}\} \leq n' \leq \max\{n_{\text{lactose}}\} \tag{3.1}$$

In Figure 3, the lactose crystals are mounted in an refractive index liquid with $n_{\text{m}} = 1.570$. As observed in the figure, the Becke lines move out from the crystals as the depth of focus is moved in the direction of the illuminating light, *i.e.*, towards

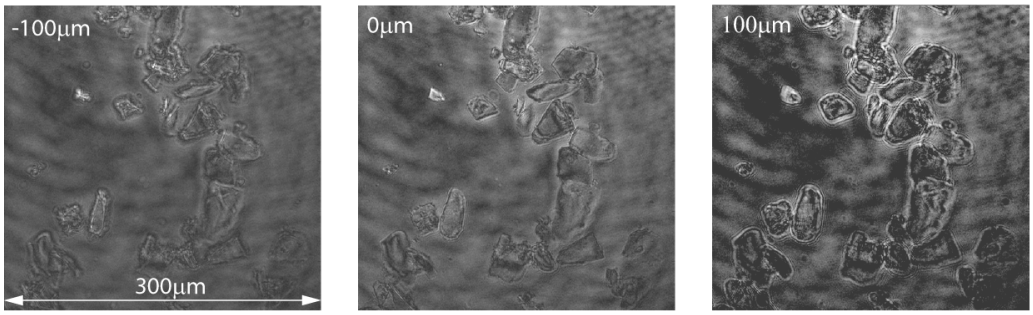

Figure 3: Amplitude images of lactose crystals mounted in a liquid with $n_{\mathrm{m}} = 1.570$. The Becke lines move out from the crystals into the liquid as the image plane is shifted in the direction of the illuminated wave, *i.e.*, towards the sensor from $-100\,\mu$m to $100\,\mu$m.

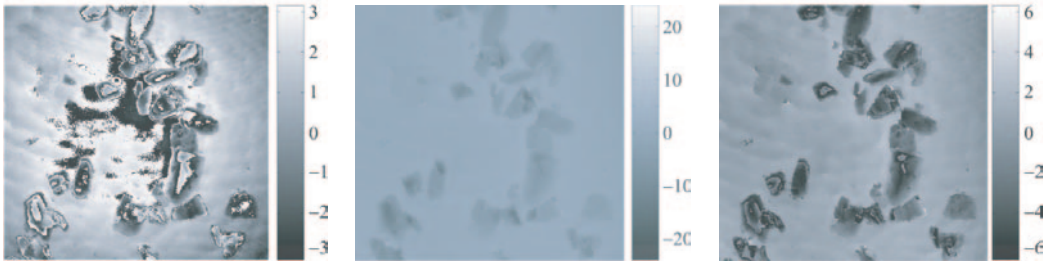

Figure 4: Phase images of lactose crystals mounted in a liquid with $n_{\mathrm{m}} = 1.570$. The phase decreases when going from the liquid into the crystals. a) the wrapped phase image where the color changes from white over gray to black and back to white, modulus 2π, in the crystals. b) the unwrapped phase image. c) the re-wrapped phase image.

the sensor from $-100\,\mu$m to $100\,\mu$m. The refractive index of the liquid is hence larger than the refractive index of the crystal, *i.e.*, $n' \leq n_{\mathrm{m}}$ for all crystals.

In Figure 4, phase images corresponding to the amplitude image in Figure 3b are shown. The phase delay is observed as a color change from white over gray to black and back to white, *i.e.*, in the negative direction, in the wrapped phase image. Even though the wrapped phase image contain the necessary information about the phase variation it is not a convenient way to present the results. The wrapped phase image also suffers from an uneven illumination, *i.e.*, both the small scale phase variation of the crystals and the large scale phase variation of the illumination light is shown in the wrapped phase image.

The wrapped phase image in Figure 4a is improved noticeably by a two-dimensional phase unwrapping. Here, the Flynn's minimum discontinuity algorithm is used [3]. In Figure 4b, the unwrapped phase image is shown. The large scale phase variation of the illuminating wave is removed by fitting the unwrapped phase image

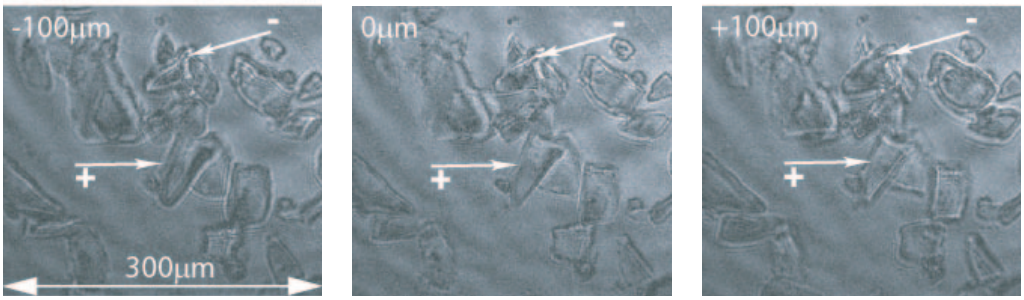

Figure 5: Amplitude images of lactose crystals mounted in a liquid with $n_{\mathrm{m}} = 1.542$. The Becke lines move into the regions with higher refractive index as the image plane is shifted in the direction of the illuminated wave, *i.e.*, towards the sensor from $-100\,\mu$m to $100\,\mu$m.

to a polynomial. For the results presented in this paper it has been sufficient to use a second order polynomial. Since the background is extracted from the image, the image amplitude is proportional to the contrast in refractive index times the propagation length through each crystal. Objects with positive (negative) relief is clearly visible as brighter (darker) objects. To improve the contrast of the unwrapped phase image in Figure 4c, the unwrapped phase is re-wrapped to the range -2π to 2π.

By a proper choice of the refractive index liquid it is possible to obtain a mixture of crystals with higher and lower index of refraction relative to the mounting medium, respectively. In Figure 5, the lactose crystals are mounted in a liquid with $n_{\mathrm{m}} = 1.542$. As observed in the figure, the Becke lines move into some crystals and out from other crystals as the focus is moved in the direction of the illuminating light, *i.e.*, towards the sensor from $-100\,\mu$m to $100\,\mu$m. For example, the crystal indicated by the +sign (-sign), the Becke lines move into (out from) the crystal, and hence the crystal has a positive (negative) relief. The refractive index of the liquid, n_{m}, is somewhere between the smallest and largest values of the refractive index of lactose, *i.e.*,

$$\min\{n_{\mathrm{lactose}}\} \leq n_{\mathrm{m}} \leq \max\{n_{\mathrm{lactose}}\} \tag{3.2}$$

In Figure 6a, the unwrapped phase image is shown. The background is extracted from the image so the image amplitude is proportional to the contrast in refractive index times the propagation length through each crystal. Objects with positive (negative) relief is clearly visible as brighter (darker) objects. To improve the contrast of the unwrapped phase image in Figure 6b, the unwrapped phase is re-wrapped to the range -2π to 2π.

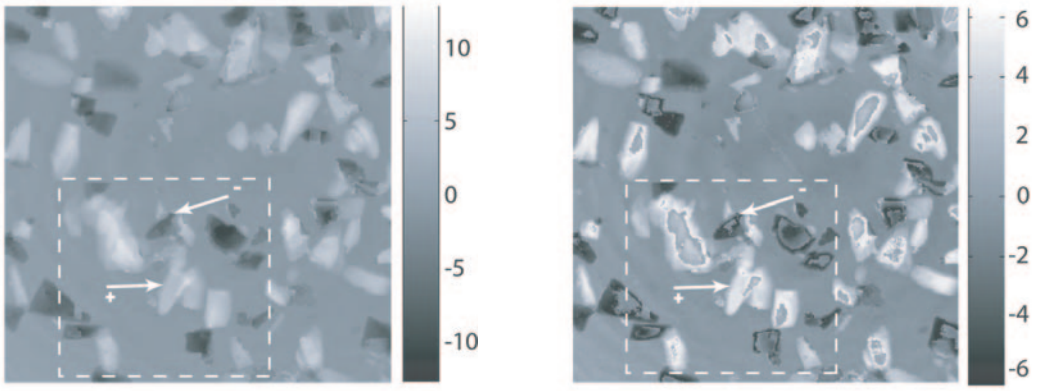

Figure 6: Phase images of lactose crystals mounted in a liquid with $n_{\mathrm{m}} = 1.542$. The phase increases (decreases) when going from an object with higher (lower) refractive index to an object with lower (higher) refractive index. a) the unwrapped phase image. b) the re-wrapped phase image.

4 Setup

The used experimental set-up is basically a Fourier type set-up where a JDS Uniphase 10 mW, 633 nm laser is divided into a reference beam and a object beam by a beam splitter. Two polarizing filters are used in conjunction with two half wave plates to adjust the intensity and the polarization in the two beams. The object beam is then directed on to the object by a 30 mm beam splitter. On the other side of the beam splitter a 0.25 pitch GRIN lens focuses the reference beam to create a reference point source. The reference point source is reflected in the beam splitter to the sensor and thus creates a virtual point source close to the object, see Figure 7. By alignment, the virtual point source can be placed arbitrary close to the object. The sensor is a Kodak KAF-3200E monochromatic CCD with 2184×1472 pixels and a pixel size of $6.8 \times 6.8\,\mu$m. The distance between the object and reference point source is typically 1 mm. To fully resolve the interference fringes the CCD is placed at a distance of about 40 mm from the object.

A common "wet mount" is used in the sample preparation. From a set of Cargille Refractive Index Liquids a suitable liquid is chosen and few drops are placed on a microscope slide. The lactose powder is sprinkled on the drops and a cover glass is placed on top enclosing the crystals surrounded by the liquid. The index of refraction of the liquids are defined at a wavelength of 589.3 nm and due to dispersion, the liquids have a slightly lower index of refraction at the wavelength of 632.8 nm used in the experiments. However, this have no effect on the results in this paper as they only depend on the sign of the relief, *i.e.*, if the object has higher or lower index of refraction than the surrounding liquid, and hence no exact value is necessary. This also applies to the temperature coefficient where the liquids have a lower index of refraction at higher temperatures.

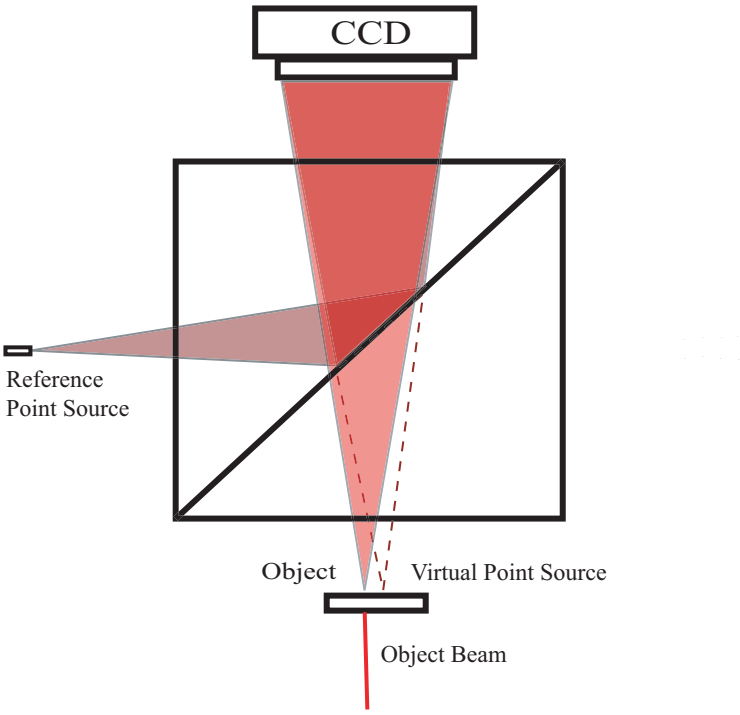

Figure 7: The digital Fourier holographic setup. A beam splitter reflects the reference point source which creates a virtual point source close to the object.

5 Discussion and conclusions

In this paper, DH is used to image small inhomogeneous objects with a resolution comparable to traditional microscopy. The additional information given by holography is used in refractometric measurements of these objects. The Becke line method is simplified as only one set of exposures is needed to image the object on all depths of focus. This gives the possibility to save the hologram and at a later time and another place study the movements of the Becke lines. Phase imaging of the objects gives another dimension to refractometric measurements. When extracting the phase from the holographic images an alternative method of separating objects with different indexes of refraction is shown.

The index of refraction of an isotropic object can be determined with both methods with repeated measurements where the liquid is changed until no relief is visible. The phase method is convenient in these types of measurements since the contrast between the indexes of variation is seen directly in the images. Two different isotropic objects can be separated if the surrounding liquid is matched somewhere between the indexes of refraction of the two objects. With multiple measurements three or more different objects can also be separated with this method.

Anisotropic objects have different index of refraction in different directions. As described above, the co-polarized part of the scattered light from a anisotropic object seems to have been scattered by an isotropic object with a effective index of refraction n'. By multiple exposures of the same object, with a step by step rota-

tion of the polarization of the illuminating light, the smallest and the largest of the principal refractive indexes can be extracted. The anisotropic objects considered here are uniaxial, *i.e.*, they have one optical axis where the index of refraction varies with polarization. The thickness of the object can in this case be disregarded.

Acknowledgments

We thank Bengt Bengtsson, Peter Egelberg, Thomas Lenart, Sven-Göran Pettersson, and Viktor Öwall for many fruitful discussions about digital holography.

This work is partly funded by the Competence Center for Circuit Design (CCCD), Department of Electroscience, Lund University, Sweden and Neural AB, Sweden. Their support is gratefully acknowledged.

References

[1] M. Born and E. Wolf. *Principles of Optics*. Cambridge University Press, Cambridge, U.K., seventh edition, 1999.

[2] F. Dubois, C. Minetti, O. Monnom, C. Yourassowsky, J. C. Legros, and P. Kischel. Pattern recognition with a digital holographic microscope working in partially coherent illumination. *Appl. Opt.*, **41**(20), 4108–4119, July 2002.

[3] D. C. Ghiglia and M. d. Pritt. *Two-Dimensional Phase Unwrapping: theory, algorithms, and software*. John Wiley & Sons, New York, 1998.

[4] M. Gustafsson, M. Sebesta, B. Bengtsson, S.-G. Pettersson, P. Egelberg, and T. Lenart. High resolution digital transmission microscopy—a Fourier holography approach. Technical Report LUTEDX/(TEAT-7106)/1–11/(2002), Lund Institute of Technology, Department of Electroscience, P.O. Box 118, S-211 00 Lund, Sweden, 2002. Accepted by Optics and Lasers in Engineering, doi:10.1016/S0143-8166(02)00214-2.

[5] M. Jacquot, P. Sandoz, and G. Tribillon. High resolution digital holography. *Optics Communcations*, **190**, 87–94, 2001.

[6] W. D. Nesse. *Introduction to optical Mineralogy*. Oxford University Press, New York, second edition, 1991.

[7] U. Schnars and W. P. O. Jüptner. Digital recording and numerical reconstruction of holograms. *Meas. Sci. Technol*, **13**, R85–R101, 2002.

[8] S. Seebacher, W. Osten, T. Baumbach, and W. Jüptner. The determination of material parameters of microcomponents using digital holography. *Optics and Lasers in Engineering*, **36**, 103–126, 2001.

[9] W. Xu, M. H. Jericho, I. A. Meinertzhagen, and H. J. Kreuzer. Digital in-line holography for biological applications. *Cell Biology*, **98**(20), 11301–11305, September 2001.